J. Eukaryot. Microbiol., 47(3), 2000 pp. 264–270

Ultrastructural Distribution of Poly (A)$^+$ RNA During *Trypanosoma cruzi*–Cardiomyocyte Interaction in vitro: A Quantitative Analysis of the Total mRNA Content by in situ Hybridization

MIRIAN CLAUDIA S. PEREIRA,[a] ROBERT H. SINGER[b] and MARIA DE NAZARETH S. L. DE MEIRELLES[a]

[a]*Departamento de Ultra-estrutura e Biologia Celular, Instituto Oswaldo Cruz, FIOCRUZ, Av. Brasil 4365, 21045-900, Rio de Janeiro, Brazil, and*

[b]*Department of Anatomy and Structural Biology and Cell Biology, Albert Einstein College of Medicine, Bronx, New York 10461, USA*

ABSTRACT. Ultrastructural in situ hybridization was used to visualize the spatial distribution of poly (A)$^+$ RNA and quantitate its relative amount within different cellular compartments of cardiomyocytes after *T. cruzi* infection. The amount of poly (A)$^+$ RNA remained about the same up to 24 h post-infection. In contrast, its content was reduced 65% after 72 h of interaction, showing a marked decrease in the cell cytoplasm. This decline in poly (A)$^+$ RNA level in host cell cytoplasm was concomitant with intracellular proliferation of *T. cruzi* amastigotes. Thus, *T. cruzi* may affect host cell cytoplasmic mRNA stability, associated with the parasite's intracellular multiplication.

Key Words. Chagas' disease, heart muscle cells, hemoflagellate, ultrastructural in situ hybridization.

TRYPANOSOMA cruzi, the causative agent of Chagas' disease, invades and multiplies within most vertebrate cells in vitro. Several studies have focused on the biological and molecular processes involved during the *T. cruzi*-host cell's interaction, aiming for a better understanding of the clinical disease (Campos de Carvalho et al. 1994; Tanowitz et al. 1996; Vermelho et al. 1997). Previous reports have shown that *T. cruzi* minicircle kDNA can be integrated into the host cell genome, suggesting that this parasite may interfere with the cell synthesis machinery (Teixeira et al. 1994). Several lines of evidence indicate that *T. cruzi* infection alters the host cell gene expression in lymphocytes (Lopez et al. 1993; Majumder and Kierszenbaum 1995; Soong and Tarleton 1992). However, the understanding of the mechanism by which the parasites evoke these anomalies remains limited.

Despite the fact that cardiomyopathy is a serious clinical symptom in Chagas' disease, very little is known about the molecular alterations that this hemoflagellate parasite induces in cardiomyocytes. Using an in vitro system of mouse embryo cardiomyocytes, several molecules involved in the *T. cruzi*-heart muscle cell recognition process have been identified (Araújo-Jorge, Barbosa, and Meirelles 1992; Barbosa and Meirelles 1992, 1993). This parasite-cell interaction modulates the expression of cardiomyocyte surface components, playing an important role in the parasite internalization process (Soeiro, Silva e Filho, and Meirelles 1995; Vermelho et al. 1992). The parasites may also disrupt the heart muscle cell contractile apparatus and alter the cytoskeleton (Pereira et al. 1993). More recently, we have demonstrated that *T. cruzi* affects actin mRNA regulation in heart muscle cells (Pereira et al. unpubl. data), providing the first evidence of actin mRNA cytoplasmic delocalization by pathological mechanisms.

The purpose of the present study was to evaluate possible changes in total poly (A)$^+$ RNA during *T. cruzi*-cardiomyocyte interaction. The cellular distribution of poly (A)$^+$ RNA was analyzed by immunofluorescence and ultrastructural in situ hybridization, which revealed a reduction of 65% in the relative amount of poly (A)$^+$ RNA in highly infected cells. This reduction was more evident in the cell cytoplasm, indicating that RNA transcription still occurs in infected cells and that its degradation may be induced by the intracellular parasites.

MATERIALS AND METHODS

Cell culture. Heart muscle cells (HMC) were isolated from 18-day-old mouse embryos as previously described (Meirelles et al. 1986). Cardiac fragments were dissociated in phosphate-buffered saline (PBS) containing 0.025% trypsin plus 0.01% collagenase and plated (5–8 $\times$ 10^5 cells/ml) into 35-mm culture dishes or (1 $\times$ 10^6 cells/ml) 100-mm culture dishes containing glass coverslips. Both dishes were previously coated with 0.01% gelatin. The culture medium consisted of Dulbecco's Modified Eagle Medium (DMEM) supplemented with 10% horse serum, 5% fetal bovine serum, 2.5 mM $CaCl_2$, 1 mM L-glutamine, and 2% chicken embryo extract. The cell cultures were maintained at 37 °C in a 5% CO_2 atmosphere. After 24 h of incubation, most cells were beating spontaneously and synchronously.

Parasites. Bloodstream trypomastigote forms of *Trypanosoma cruzi*, Y strain, were obtained from Swiss Webster mice at the peak of the parasitemia as described (Meirelles, Souto-Padrón, and de Souza 1984). Muscle cell cultures were infected at a multiplicity of infection of 10 parasites per host cell. After 24 h, free trypanosomes in the medium were removed by washing the cultures with Ringer's solution and fresh medium was added to the culture plates. The time course of infection was interrupted after 24, 48, and 72 h.

Post-embedding electron microscopy methodology. Lowicryl embedding procedure was performed as previously described (Bendayan 1983). Normal and *T. cruzi*-infected cells were fixed for 1 h at 4 °C in 4% paraformaldehyde (PFA) plus 0.01% glutaraldehyde (GA) in 0.1 M cacodylate buffer containing 3.5 M sucrose and 0.2% picric acid, pH 7.2. After fixation and successive washes, the cell cultures were incubated with PBS containing 0.5 M NH_4Cl for 30 min at 4 °C to quench free aldehyde groups. After PBS washes, they were dehydrated through an ascending series of methanol before infiltration with Lowicryl K4M (Polysciences, Inc., Warrington, PA). Lowicryl embedding was performed in an appropriate UV light container and polymerization took place for 5 d at −20 °C followed by 2 d at room temp. (22 °C).

In situ hybridization. For fluorescence in situ hybridization (FISH), cells grown on coverslips were fixed at room temp. for 10 min in 4% PFA in PBS containing 5 mM $MgCl_2$. After PBS washes, the cells were permeabilized with 0.5% Triton X-100 in PBS for 15 min. The excess of detergent was removed by three washes in PBS and then it followed pre-hybridization in 10% formamide/2× SSC (0.03 M sodium citrate and 0.3 M NaCl) at room temp. for 10 min. The cells were hybridized with 10 ng of digoxigenin-labeled oligothymidilic acid (43 nucleotides; oligo dT_{43}) probe, diluted in 10% formamide/2× SSC containing 20 mM sodium phosphate, 10 mM vanadyl complex, 1% bovine serum albumin (BSA), 10% dextran sulfate, sonicated salmom sperm DNA (10 μg), and *Escherichea coli* tRNA

Corresponding Author: M. Pereira—Telephone number: (5521) 598-4330; FAX number: (5521) 260-4434; Email: mirian@gene.dbbm.fiocruz.br

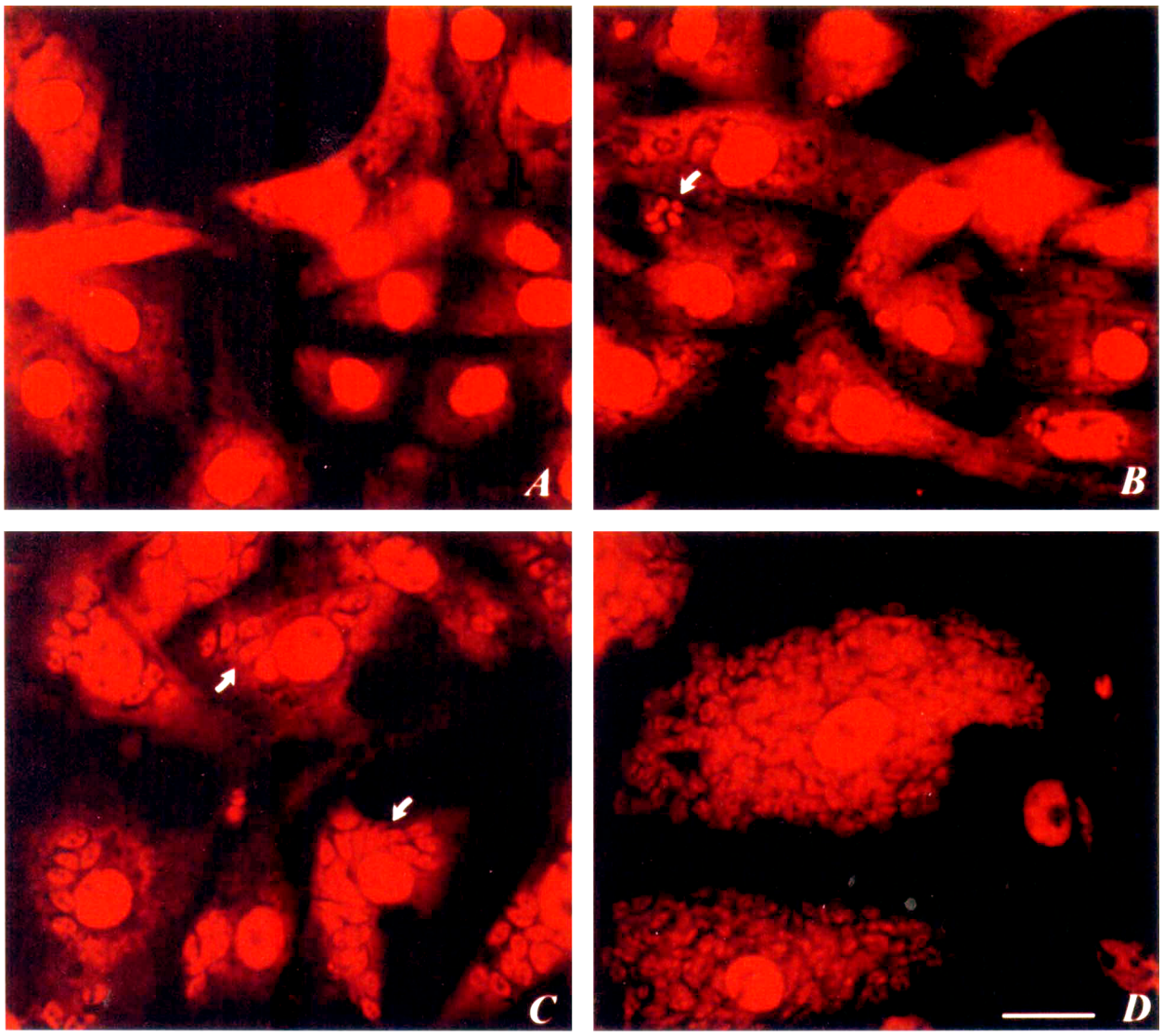

Fig. 1. Visualization by fluorescence in situ hybridization of poly (A)$^+$ RNA distribution in uninfected and *Trypanosoma cruzi*-infected cardiomyocytes. Poly (A)$^+$ RNA was detected by using Cy3-labeled oligo (dT) probe. (**A**) An intense poly (A)$^+$ signal was observed in the nucleus and cytoplasm of control cells. (**B, C**) No change in poly (A)$^+$ signal was detected 24–48 h post-infection with *T. cruzi*. (**D**) Host cell cytoplasmic poly (A)$^+$ RNA signal was weaker in 72-h infected cells, while nuclear poly (A) was not affected by infection. Note the poly (A)$^+$ signal in the intracellular parasites (arrows). Bar = 20 μm.

(10 μg) at 37 °C or 3 h in a moist chamber. After hybridization, cells were washed in 10% formamide in 2× SSC at 37 °C for 20 min, and then with 2× SSC, 1× SSC, and PBS at room temp. for 10 min each. Coverslips were mounted in 1.4-diazabicyclo-(2.2.2)-octane (DABCO; Sigma Chemical Co., St. Louis, MO) in PBS and examined immediately with a Zeiss photomicroscope equipped with epifluorescence.

For high resolution in situ hybridization, thin sections (60–80 nm) of Lowicryl- embedded samples were collected on nickel grids. For washing and incubation procedures, the grids were floated on 20-μl drops of the appropriate solution. The grids were first washed in 2× SSC and then equilibrated in 10% formamide/2× SSC containing 20 mM sodium phosphate, pH 7.0 at room temp. for 10 min each. Afterwards, they were hybridized as described above using digoxigenin-labeled probe. After hybridization, the grids were washed in 10% formamide in 2× SSC, 2× SSC, 1× SSC (20 "dips" each), and then incubated at 37 °C for 1 h with a 10 nm gold-conjugated sheep anti-digoxigenin antibody (Bio Cell Research Laboratories, Rancho Dominguez, CA) (1:50 dilution) in 1% BSA in 1× SSC. Afterwards, sections were post-fixed in 2% GA in 1× SSC at room temp. for 3 min, and stained with saturated uranyl acetate and Reynold's lead citrate. Oligodeoxyadenylic acid (oligo dA_{43}) was used as a negative control for in situ hybridization. The samples were examined in a Philips 400 transmission electron microscope.

Quantitative analyses of poly (A) RNA signal in electron micrographs. Ultrastructural quantitation was performed using a morphometric computing software (NIH Image 1.57). Photographs of 10 cells from each of three experiments were analyzed and the area was computed using internal markers and the magnification of the print. Colloidal gold particles were manually counted within each area marked by the computer. Hybridization was detected as single or clusters of gold parti-

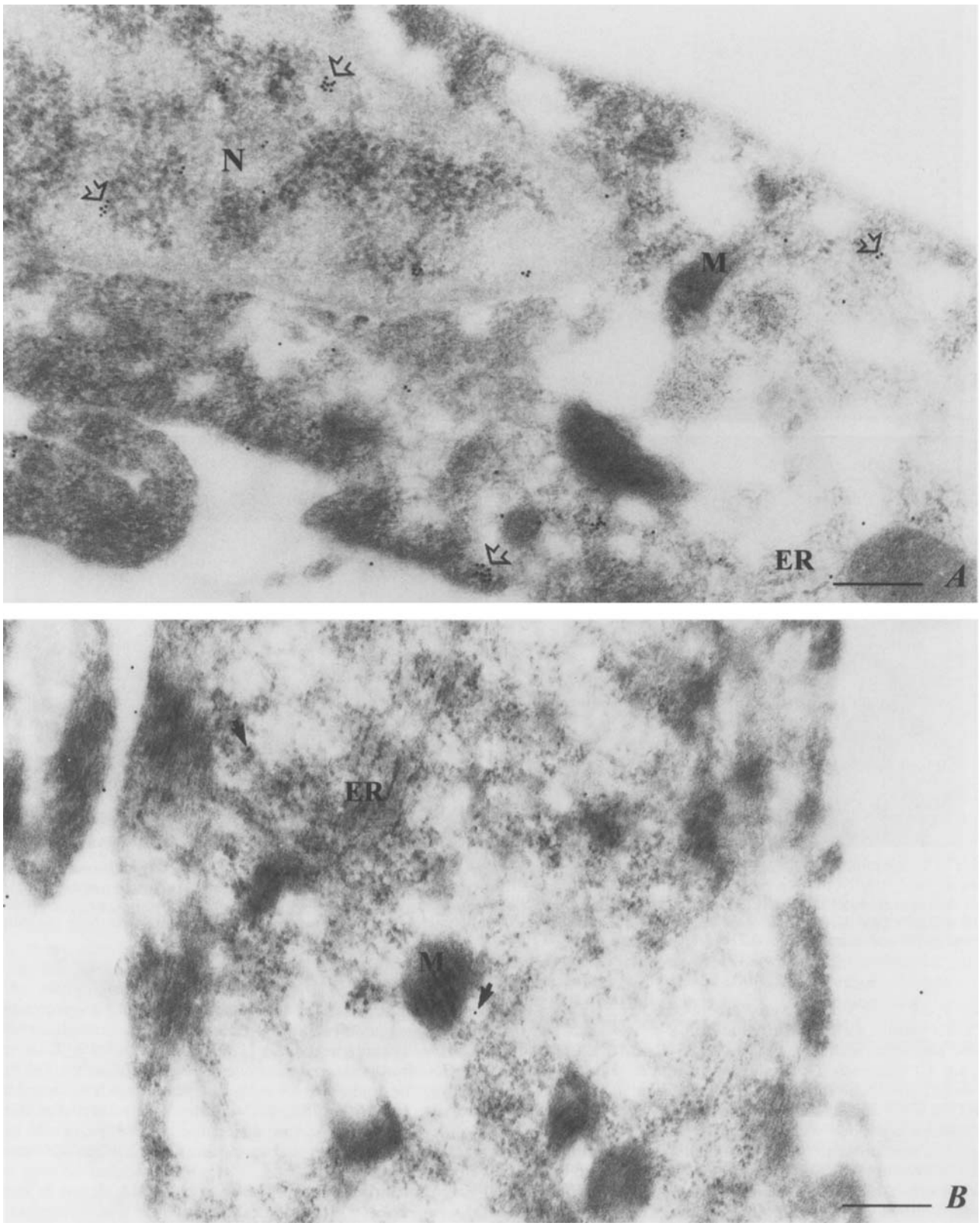

Fig. 2. Spatial distribution of poly $(A)^+$ RNA in cardiomyocytes using in situ hybridization on Lowicryl-embedded thin sections. (**A**) Single particles and clusters of 10-nm colloidal gold particles (arrows) were visualized in the nucleus (N) and cytoplasm of cardiomyocytes. (**B**) Oligo $(dA)_{43}$ probe, used as a negative control, showed few colloidal gold particles. ER, endoplasmic reticulum; M, mitochondria. Bar = 0.25 μm.

Table 1. Quantitation of poly (A)$^+$RNA distribution (colloidal gold particles/μm^2) within distinct regions of uninfected and *Trypanosoma cruzi*-infected cardiomyocytes.

	Nucleus	Cytoplasm	Mitochondrial	Total density of particles
Uninfected cells	6.54 ± 1.33	4.03 ± 0.2	6.71 ± 0.25	17.28 ± 1.87
24 h infected cells	6.37 ± 0.7	4.69 ± 0.94	4.32 ± 0.61[a]	15.38 ± 2.73
72 h infected cells	4.7 ± 0.94	1.25 ± 0.29[b]	—	5.95 ± 0.85[c]

* Student's *t*-test:
[a] $p < 0.0072/t = 2.35$
[b] $p < 0.0002/t = 2.13$
[c] $p < 0.0003/t = 2.13$.

cles. Signal-to-noise ratios (oligo dT_{43}/oligo dA_{43} signal) were also evaluated. A student's *t*-test was used to determine the statistical significance of the observed differences ($p \leq 0.05$).

RESULTS

A Cy3-labeled oligo $(dT)_{43}$ probe detection revealed an intense signal within the nucleus and cytoplasm of uninfected cells (Fig. 1). Poly (A)$^+$ RNA was uniformly distributed within the nucleus, showing discrete punctuated signal. No labeling was detected in the nucleoli. The cell cytoplasm displayed an intense signal around the nucleus, which became less intense at the cell periphery due to the low cytoplasmic density in this region (Fig. 1A).

To analyze the poly (A)$^+$ RNA distribution in *T. cruz*-infected cells, a kinetic study of host cell-parasite interaction was undertaken, providing a time-dependent analysis of total intracellular RNA distribution. After 24 and 48 h of infection, the distribution of poly (A)$^+$ RNA was similar to that of uninfected cells (Fig. 1B,C). Intracellular parasites displayed an intense cytoplasmic labeling but lower signal at the nucleoplasm. Even highly infected cells revealed a very intense poly (A)$^+$ hybridization signal, which was related to the high amount of intracellular parasites (Fig. 1D). Host cell oligo $(dT)_{43}$ hybrids were detected only in cytoplasmic areas where parasites were absent. At all time points the host cell nuclear signal was intense, indicating that the mRNA polyadenylylation process still occurs in infected cells. It was not possible to quantitate fluorescence labeling during parasite-host cell interaction due to the high fluorescence levels of intracellular parasites.

Ultrastructural localization of poly (A)$^+$ RNA demonstrated that colloidal gold particles were dispersed throughout the nucleus and cytoplasm, as well as in organelles of uninfected cells (Fig. 2). Single or clusters of colloidal gold particles were observed associated with dense chromatin within the nucleoplasm (Fig. 2A). Occasionally, it was possible to visualize poly (A)$^+$ RNA localized close to the nuclear envelope, which suggested that mRNA could be in the process of export through the nuclear pore complex to the cell cytoplasm. Large amounts of colloidal gold particles showed a random distribution in the cytoplasm (Fig. 2A). In addition to mitochondrial labeling, gold particles were also observed to colocalize with polysomes associated with rough endoplasmic reticulum profiles, which may be indicative of active translation. The background levels revealed very few gold particles in uninfected and in *T. cruzi*-infected cells hybridized with oligo $(dA)_{43}$ (Fig. 2, 3C).

Infected cells displayed no substantial change in total poly (A)$^+$ RNA distribution after 24 h of infection (Fig. 3A). Oligo $(dT)_{43}$ hybrids were also detected in large amounts within the nucleus, cytoplasm, and kinetoplast of the intracellular parasites. As the parasites replicated within the muscle cell cytoplasm, the host cell intracellular poly (A)$^+$ RNA signal seemed to be reduced. In contrast, high amounts of colloidal gold particles were observed in the replicative forms of *T. cruzi*. At 72 h, several cells already presented intracellular trypomastigote forms of *T. cruzi* with a lower poly (A)$^+$ signal (Fig. 3B).

Gold density quantitation demonstrated an average signal-to-noise ratio of > 9:1 and > 24:1 from single and multiple gold particle detection, respectively. Poly (A)$^+$ signal was frequently detected as a single particle (72%), but clusters containing more than five particles were also observed. In order to avoid error in the quantitation of poly (A)$^+$ RNA content of *T. cruzi*-infected cells, the intracellular parasite area was analyzed separately from the host cell cytoplasmic area. The kinetics of the interaction between *T. cruzi*-heart muscle cells revealed slight changes in colloidal gold particles/μm^2 after 24 h of interaction. The mitochondrial poly (A)$^+$ RNA signal was significantly decreased ($p < 0.0072$; $t = 2.35$) at 24 h (Table 1). In contrast, a reduction of 65% in total gold particles/μm^2 was observed 72 h post-infection (Table 1). A difference in the hybridization signal was observed between the host cell nucleus and cytoplasm: the poly (A)$^+$ signal was more significantly reduced in the cell cytoplasm (69%) ($p < 0.0002$; $t = 2.13$) as compared to the host cell nucleus (28%) after 72 h of *T. cruzi* interaction (Table 1). In addition, the quantitative analysis demonstrated a significant difference ($p < 0.01$ / $t = 2.13$) in the level of poly (A)$^+$ hybridization during the parasite differentiation process. In early stages of infection (24 h) when amastigote forms of *T. cruzi* were dividing, the poly (A)$^+$ RNA hybridization was 2.9 and 1.7-fold higher in the parasite nucleus and cytoplasm, respectively, compared to levels found in the intracellular trypomastigote forms at 72 h post-infection (Fig. 4).

DISCUSSION

Fluorescence in situ hybridization (FISH) using CY3 labeled oligo $(dT)_{43}$ demonstrated an intense signal within the nucleus and cytoplasm of cardiomyocytes. The nuclear poly (A)$^+$ RNA pattern has been previously reported (Carter, Taneja, and Lawrence 1991). The cytoplasmic poly (A)$^+$ RNA distribution was similar to the observations previously described in chicken fibroblasts (Taneja et al. 1992), showing an intense perinuclear signal and weaker labeling at the cell edge. In infected heart muscle cells, although the poly (A)$^+$ RNA signal seemed to be reduced after 72 h of infection, it was not possible to evaluate its relative amount due to the high signal of intracellular parasites.

We found poly (A)$^+$ RNA associated with dense chromatin within the nuclear matrix. We also visualized poly (A)$^+$ RNA in intimate association with the nuclear envelope, suggesting the transport of poly (A)$^+$ RNA through the nuclear pore complex. The detection of poly (A)$^+$ RNA in interchromatin and perichromatin granules has been also reported in Hela cells (Huang et al. 1994; Visa et al. 1993). Our results also revealed poly (A)$^+$ RNA randomly distributed in the cell cytoplasm, showing close association with endoplasmic reticulum and also

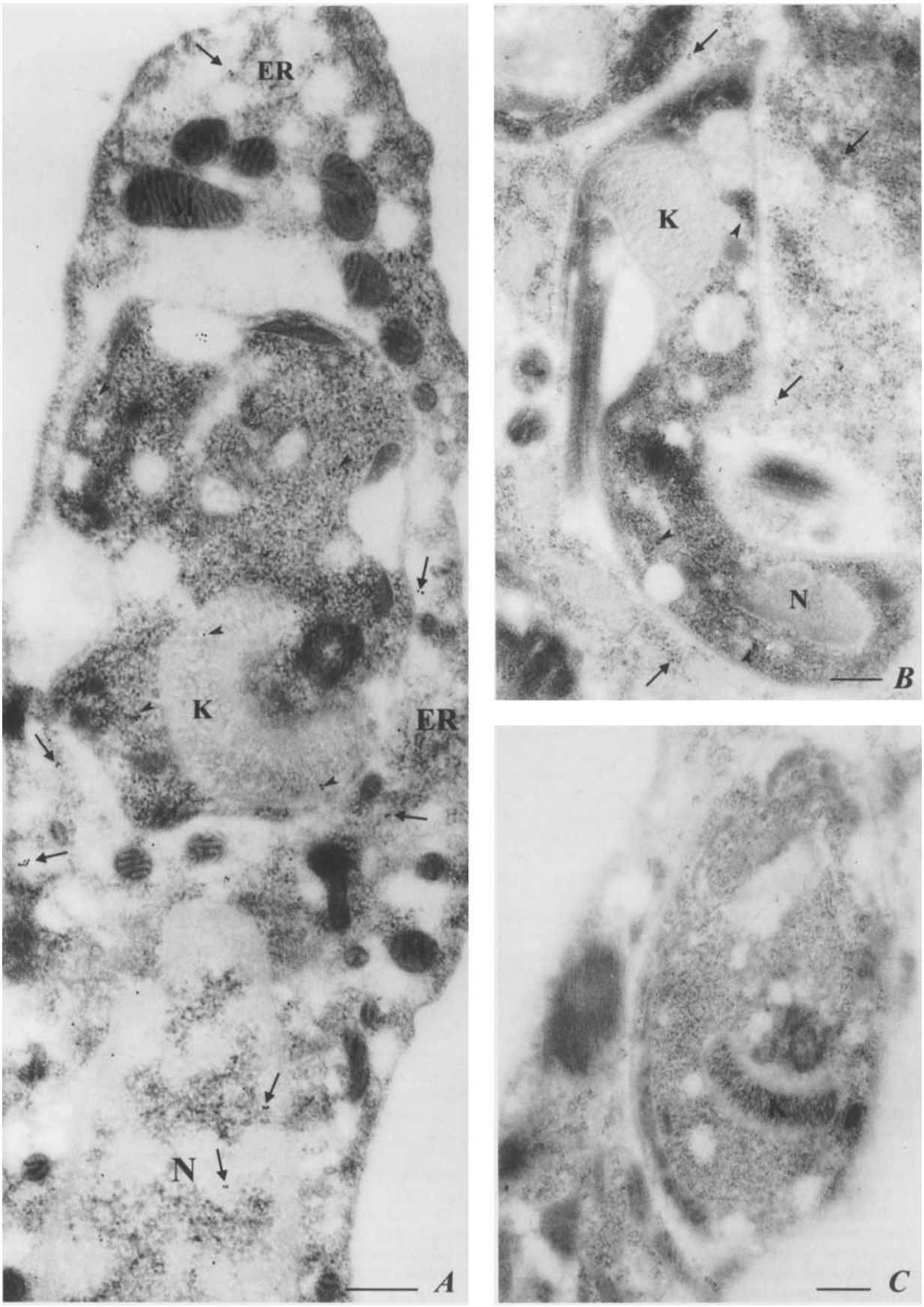
ER
K
ER
N
A
K
N
B
K
C

localized within mitochondria, as also described by others investigators (Bassel et al. 1994; Escaig-Haye et al. 1991; Topper, Van Etten, and Clayton 1983).

Ultrastructural in situ hybridization has been extensively used to quantitate poly $(A)^+$ RNA or specific mRNAs in different intracellular compartments (Bassel et al. 1994; Krause et al. 1994; Pikó and Clegg 1982). Measurements of the poly $(A)^+$ RNA amounts in 24 h *T. cruzi*-infected cells showed a slight difference in the density of gold particles/μm^2, due to a significant decrease in the poly $(A)^+$ RNA amounts in mitochondria relative to the nucleus and cytoplasm. This indicates that nuclear and cytoplasmic concentration of poly (A) (per unit area) remained mostly constant, suggesting that RNA transcription and its transport to the cytoplasm was effective despite the presence of the intracellular parasites. However, the meaning of the lower level of poly $(A)^+$ RNA in mitochondria is not clear. On the other hand, demonstration that poly $(A)^+$ RNA amount is reduced 65% after 72 h of infection and that the cytoplasmic labeling was highly affected, showing a decrease of 69% in the poly $(A)^+$ RNA signal indicate that the high amount of intracellular parasites may not interfere directly with the RNA transcription, but may alter mRNA stability.

It has been demonstrated that different trypanosomatid flagellates, including *Leishmania* and *Trypanosoma*, are unable to synthesize their own source of purines. Instead, they depend on exogenous supplies of host-derived preformed purines (Kidder and Dutta 1958; Marr, Berens, and Nelson 1978). The 3′- and 5′-nucleotidase enzymes, which are capable of hydrolysing both 3′-ribonucleotides and nucleic acids, have been identified in the surface membrane of several trypansomatids, indicating their involvement in purine acquisition by the parasites (Côrte-Real, Porrozzi, and Meirelles 1993; Gottlieb 1985; Gottlieb 1989; Gottlieb, Gardiner, and Dwyer 1986). Besides the presence of 5′-nucleotidase in the *T. cruzi* surface (Nagakura et al. 1986), the catabolic pathway of thymidine phosphorylase, which degrades thymine nucleotides to thymine, has also been described in *T. cruzi* (Al Cahlabi and Gutteridge 1977). Thus, the nuclease activity of these intracellular parasites may be one of the mechanisms responsible for the reduction of host cell poly $(A)^+$ RNA.

Our study also revealed changes in the level of poly $(A)^+$ RNA during the parasites' intracellular cycle. An increase in poly $(A)^+$ RNA in intracellular amastigote forms (dividing form) and subsequent decrease after differentiation into trypomastigotes indicates a progressive enhancement in RNA content during the parasites' intracellular proliferation. Similar results were obtained during *Trypanosoma brucei* differentiation (Pays et al. 1993), where an abrupt RNA change occurred during the differentiation of bloodstream forms into procyclic forms in vitro.

In conclusion, host cell total poly $(A)^+$ RNA was significantly reduced in the cytoplasm of highly infected cells, suggesting that *T. cruzi* infection affects poly $(A)^+$ RNA stability. Interestingly, the increase in poly $(A)^+$ RNA level in the parasites seems to be simultaneous with its decline in the host cell cytoplasm, which suggests that the host cell mRNA degradation may be induced by intracellular parasites during their multiplication process. However, the mechanisms involved in the RNA degradation process are still unknown and will be the focus of future investigations.

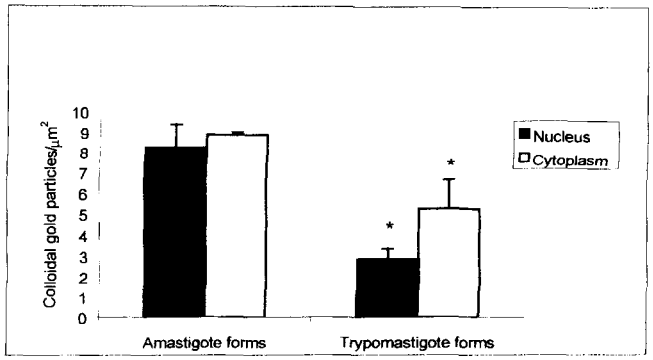

Fig. 4. Quantitative analysis of poly $(A)^+$ RNA level by high resolution in situ hybridization during intracellular differentiation of *Trypanosoma cruzi* using oligo $(dT)_{43}$ hybridization within the nucleus and cytoplasm of amastigotes and trypomastigotes. High levels of poly $(A)^+$ RNA were detected in amastigotes, the proliferative forms of the parasite, while trypomastigotes showed a significantly lower level of total poly $(A)^+$ RNA in the nucleus (Student's *t*-test: $p < 0.001$ / t = 2.13) and cytoplasm (Student's *t*-test: $p < 0.01$ / t = 2.13).

ACKNOWLEDGMENTS

We thank Drs. Krishan Taneja for constructing the oligonucleotide probes and Maurilio José Soares for critical review of the manuscript, Bruno Avila for his skillful computer imaging support, Genésio Lopes de Faria, Marcos Meuser Batista, and José Lopes Faria for their technical assistance. This work has been supported by grants from Fundação Oswaldo Cruz (FIOCRUZ), Conselho Nacional de Desenvolvimento Científico e Tecnológico (CNPq) FAPERJ, PADCT/FIOCRUZ and PAPES/FIOCRUZ.

LITERATURE CITED

Al Cahlabi, K. & Gutteridge, W. E. 1977. Catabolism of deoxythymidylate in some trypanosomatids. *Parasitol.*, **74**:299–312.

Araújo-Jorge, T. C., Barbosa, H. S. & Meirelles, M. N. L. 1992. *Trypanosoma cruzi* recognition by macrophages and muscle cells: perspectives after a 15-year study. *Mem. Inst. Oswaldo Cruz*, **87**:43–56.

Barbosa, H. S. & Meirelles, M. N. L. 1992. Ultrastructural detection in vitro of WGA-, RCA I-, and Con A-binding sites involved in the invasion of heart muscle cells by *Trypanosoma cruzi*. *Parasitol. Res.*, **78**:404–409.

Barbosa, H. S. & Meirelles, M. N. L. 1993. The role of RCA-biding sites in the adhesion of *Trypanosoma cruzi* to heart muscle cells, as revealed by electron spectroscopic imaging. *J. Submicrosc. Cytol. Pathol.*, **25**:47–51.

Bassel, G. J., Powers, C. M., Taneja, K. L. & Singer, R. H. 1994. Single mRNA visualized by ultrastructural in situ hybridization are principally localized at actin filament intersections in fibroblasts. *J. Cell Biol.*, **126**:863–876.

←

Fig. 3. Ultrastructural detection of poly $(A)^+$ RNA in *Trypanosoma cruzi*-infected cardiomyocytes. Oligo (dT) hybrids were detected using 10-nm colloidal gold-labeled anti-digoxigenin antibody. (**A**) Poly $(A)^+$ RNA was detected in 24-h infected cells as single and multiples colloidal gold particles in the host cell nucleus and cytoplasm (arrows). Oligo (dT) hybridization was also detected in the intracellular amastigote form of *T. cruzi* (arrowheads). (**B**) In highly infected cells, low level of poly $(A)^+$ signal was detected in the host cell cytoplasm (arrows). (**B**) Intracellular trypomastigote forms also revealed a low level of poly $(A)^+$ RNA signal (arrowheads) as compared to the amastigote forms. (**C**) In situ hybridization with control oligo (dA) demonstrated low background levels. ER, endoplasmic reticulum; K, kinetoplast; M, mitochondrion; N, nucleus. Bar = 0.25 μm.

Bendayan, M. 1983. Ultrastructural localization of actin in muscle, epithelial cells and secretory cells by applying the protein A-gold immunocytochemical technique. *Histochem. J.*, **15**:39–58.

Campos de Carvalho, A., Masuda, M. O., Tanowitz, H. B., Wittner, M., Goldenberg, R. C. S. & Spray, D. C. 1994. Conduction defects and arrhythmias in Chagas' disease: possible role of Gap junctions and humoral mechanisms. *J. Cardiovasc. Electrophysiol.*, **5**:686–698.

Carter, K. C., Taneja, K. L. & Lawrence, J. B. 1991. Discrete nuclear domains of poly (A) RNA and their relationship to the functional organization of the nucleus. *J. Cell Biol.*, **115**:1191–1202.

Côrte-Real, S., Porrozzi, R. A. & Meirelles, M. N. L. 1993. Immunogold labeling and cerium cytochemistry of the enzyme ecto-5′-nucleotidase in promastigote forms of *Leishmania* species. *Mem. Inst. Oswaldo Cruz*, **88**:407–412.

Escaig-Haye, F., Grigoriev, V., Peranzi, G., Lestienne, P. & Fournier, J.–G. 1991. Analysis of human mitochondria transcripts using electron microscopic in situ hybridization. *J. Cell Sci.*, **110**:851–862.

Gottlieb, M. 1985. Enzyme regulation in trypanosomatids: effect of purine starvation on levels of 3′-nucleotidase activity. *Science*, **227**: 72–74.

Gottlieb, M. 1989. The surface membrane 3′-nucleotidase/nuclease of trypanosomatid protozoa. *Parasitol. Today*, **5**:257–260.

Gottlieb, M., Gardiner, P. R. & Dwyer, D. M. 1986. 3′- nucleotidase activity in procyclic and bloodstream stages of *Trypanosoma rhodesiense*. *Comp. Biochem. Physiol.*, **83B**:63–69.

Huang, S., Deerinck, T. J., Ellisman, M. H. & Spector, D. L. 1994. In vivo analysis of the stability and transport of nuclear poly (A)$^+$ RNA. *J. Cell Biol.*, **126**:877–899.

Kidder, G. W. & Dutta, B. N. 1958. The growth and nutrition of *Crithidia fasciculata*. *J. Gen. Microbiol.*, **18**:621–638.

Krause, S., Fakan, S., Karsten, W. & Wahle, E. 1994. Immunodetection of poly (A) binding protein II in the cell nucleus. *Exp. Cell Res.*, **214**:75–82.

Lopez, H. M., Tanner, M. K., Kierszenbaum, F. & Sztein, M. B. 1993. Alterations induced by *Trypanosoma cruzi* in activated mouse lymphocytes. *Parasite Immunol.*, **15**:273–280.

Majumder, S. & Kierszenbaum, F. 1995. *Trypanosoma cruzi* immunosuppressive factor decreases the interleukin-2 mRNA level in cultured normal activated human lymphocytes. *Infection and Immunity*, **63**: 4546–4549.

Marr, J. J., Berens, R. L. & Nelson, D. J. 1978. Purine metabolism in *Leishmania donovani* and *Leishmania braziliensis*. *Biochem. Biophys. Acta*, **544**:360–371.

Meirelles, M. N. L., Souto-Padrón, T. & De Souza, W. 1984. Participation of cell surface anionic sites in the interaction between *Trypanosoma cruzi* and macrophages. *J. Submicrosc. Cytol.*, **16**:533–545.

Meirelles, M. N. L., Araújo-Jorge, T. C., Miranda, C. F., De Souza, W. & Barbosa, H. S. 1986. Interaction of *Trypanosoma cruzi* with heart muscle cells: ultrastructure and cytochemical analysis of endocytic vacuole formation and effect upon myogenesis in vitro. *Europ. J. Cell Biol.*, **41**:198–206.

Nagakura, K., Tachibana, H., Kaneda, Y. & Sekine, T. 1986. Subcellular fraction of *Trypanosoma cruzi*: isolation and characterization of plasma membranes from epimastigotes. *Tokai J. Exp. Clin. Med.*, **11**:23–29.

Pays, E., Hanocq-Quertier, J., Hanocq, F., Assel, S. V., Nolan, D. & Rolin, S. 1993. Abrupt RNA changes precede the first cell division during the differentiation of *Trypanosoma brucei* bloodstream forms into procyclic forms in vitro. *Mol. Biochem. Parasitol.*, **61**:107–114.

Pereira, M. C. S., Costa, M., Chagas Filho, C. & Meirelles, M. N. L. 1993. Myofibrillar breakdown and cytoskeleton alterations in heart muscle cells during invasion by *Trypanosoma cruzi*: immunological and ultrastructural study. *J. Submicrosc. Cytol. Pathol.*, **25**:559–569.

Pikó, L. & Clegg, K. B. 1982. Quantitative changes in total RNA, total poly (A), and ribosomes in early mouse embryos. *Dev. Biol.*, **89**: 362–378.

Soeiro, M. N. C., Silva e Filho, F. C. & Meirelles, M. N. L. 1995. Alterations in the surface charge of heart muscle cells during the interaction with *Trypanosoma cruzi*. *Cell Biophysics*, **26**:21–44.

Soong, L. & Tarleton, R. L. 1992. Selective suppressive effects of *Trypanosoma cruzi* infection on IL-2, c-myc, and c-fos gene expression. *J. Immunol.*, **149**:2095–2102.

Taneja, K. L., Lifshitz, L. M., Fay, F. S. & Singer, R. H. 1992. Poly (A) RNA codistribution with microfilaments: evaluation by in situ hybridization and quantitative digital imaging microscopy. *J. Cell Biol.*, **119**:1245–1260.

Tanowitz, H. B., Kaul, D. K., Chen, B., Morris, S. A., Factor, S. M., Weiss, L. M. & Wittner, M. 1996. Compromised microcirculation in acute murine *Trypanosoma cruzi* infection. *J. Parasitol.*, **82**:124–130.

Teixeira, A. R. L., Argañaraz, E. R., Freitas Jr., L. H., Lacava, Z. G. M., Santana, J. M. & Luna, H. 1994. Possible integration of *Trypanosoma cruzi* kDNA minicircles into the host cell genome by infection. *Mutation Res.*, **305**:197–209.

Topper, D. P., Van Etten, R. A. & Clayton, D. A. 1983. Isolation of mammalian mitochondrial DNA and RNA and cloning of mitochondrial genome. *Methods Enzymol.*, **97**:426–435.

Vermelho, A. B., Barreto-Bergter, E., Pereira, M. C. & Meirelles, M. N. L. 1992. Glycolipid and protein profiles of normal and *Trypanosoma cruzi*-infected heart muscle cells. *Acta Tropica*, **52**:17–25.

Vermelho, A. B., Meirelles, M. N. L., Pereira, M. C., Pohlentz, G. & Barreto-Bergter, E. 1997. Heart muscle cells share common neutral glycosphingolipids with *Trypanosoma cruzi*. *Acta Tropica*, **64**:131–143.

Visa, N., Puvion-Dutilleul, F., Harper, F., Bachellerie, J. P. & Puvion, E. 1993. Intranuclear distribution of poly (A) RNA determined by electron microscope in situ hybridization. *Exp. Cell Res.*, **208**:19–34.

Received: 6-18-99, 10-28-99, 12-16-99, 1-6-00; accepted 1-6-00